# Anomalous diffusion

December 8, 2000

In this lecture we discuss stochastic models of correlated random walks. By "correlated" we mean that that if a particle is headed in one direction then there is nonzero probability that it continues in that same direction for some time and this probability fades to zero as the time interval increases. This is, of course, the situation envisaged by Taylor (1921).

The distinction between normal and anomalous diffusion made in lecture 1 can be understood by examining the rate at which velocity correlation decrease to zero. Normal diffusion occurs if the velocity correlation decrease rapidly while anomalous diffusion results from processes in which particles move coherently for long times with infrequent changes of direction. Roughly speaking, this distinction is quantified by the tail behaviour of the velocity autocorrelation function. For example, if the correlation function decays exponentially then there is normal diffusion, whereas if the correlation function decays algebraically then there is the possibility of anomalous diffusion.

The definition of anomalous diffusion is based only on the behaviour of the second moment, $\langle x^2 \rangle$. But we usually want to know more about the distribution of a tracer than simply the second moment. In the case of normal diffusion, detailed information concerning the tracer distribution is obtained by solving the diffusion equation

$$c_t = D c_{xx} \, . \tag{1}$$

Can we obtain continuum models, analogous to (1), which provide the same detailed information for anomalously diffusing tracer? The main goal of this lecture is to develop partial differential equation models which can be used for this purpose.

# 1 Superdiffusion and subdiffusion

## 1.1 Taylor's formula and long tails

Yet again we recall Taylor's formula which relates the growth of position variance to an integral of the Lagrangian velocity autocorrelation function, $\mathrm{corr}(t)$,

$$\frac{\mathrm{d}\langle x^2\rangle}{\mathrm{d}t} = 2\int_0^t \mathrm{corr}(t')\,\mathrm{d}t'\,. \tag{2}$$

In order to obtain $\langle x^2\rangle$ we must integrate (2). Standard manipulations turn the resulting double integral of $\mathrm{corr}(t)$ into a single integral

$$\langle x^2\rangle = 2\int_0^t (t-t')\mathrm{corr}(t')\,\mathrm{d}t'\,. \tag{3}$$

The result (3), which is not in Taylor's original paper, will prove to be very useful.

We usually have in mind situations in which $\mathrm{corr}(t)$ decreases to zero as $t\to\infty$ so that the integrals in (2) and (3) converge to nonzero values. An example is the renovating wave model, with its "triangular" correlation function, from lecture 2. Later in this lecture I will introduce the telegraph model which has an exponentially decaying correlation function, $\mathrm{corr}(t) = U^2\exp(-2\alpha t)$. These are both examples in which correlations decrease very rapidly so that normal diffusion occurs. But now consider the possibility that $\mathrm{corr}(t)$ decreases so slowly that the integrals in (3) diverge.

Suppose, for instance, that as $t\to\infty$, $\mathrm{corr}(t)\sim t^{-\eta}$ with $0<\eta<1$. Even though the diffusivity no longer exists, it still follows from (3) that

$$\langle x^2\rangle \sim t^{2-\eta}\,. \tag{4}$$

In this case there is *superdiffusion*: the variance of the particle displacement grows faster than linearly with time because $2-\eta>1$.

Taylor's formula also contains the possibility of *subdiffusion*. This case is subtle because, like the example of the sea-surface mentioned in lecture 1, it requires that the integral defining $D$ is zero. But suppose additionally that the remaining integral in (3) diverges. This can happen if $\mathrm{corr}(t)\sim ct^{-\eta}$ with $1<\eta<2$. The condition that $1<\eta$ ensures that $\int_0^\infty \mathrm{corr}(t')\,\mathrm{d}t'$ converges (to zero). The second inequality, $\eta<2$, ensures that $\int_0^t t'\mathrm{corr}(t')\,\mathrm{d}t'$ diverges.

Using (3), we again find the scaling law in (4). However this time, because $2 - \eta < 1$, there is *subdiffusion*.

At first glance two possibilities above appear as unlikely exceptions to the more natural cases in which both integrals in (3) converge. However there are examples in fluid mechanics in which either subdiffusion or superdiffusion is observed experimentally or computationally. Thus (4) cannot be dismissed as an unlikely pathology.

## 1.2 The Texas experiments

An experiment illustrating anomalous diffusion has been conducted in Swinney's laboratory at University of Texas; see Solomon, Weeks & Swinney (1994) and Weeks, Urbach & Swinney (1996). These investigators study the dispersion of particles in an almost two-dimensional flow in annular tank (see figure 1). The tank is rotating at about 1 or 2 Hertz and the bottom is sloped to simulate the $\beta$-effect. Because of the rapid rotation the flow is quasi two-dimensional.

The flow is forced by pumping fluid through the tank. If the pumping rate is sufficiently large then this azimuthal flow is unstable to a vortex-forming instability. A typical flow pattern in the rotating frame is shown in figure 2. Evident also in this figure is the azimuthal jet which runs all the way around the tank. The vortex pattern can be perturbed experimentally by making the strength of the pumping depend on azimuth. In this fashion, one can drive an unsteady flow and observe chaotic particle trajectories.

Automated image processing techniques are used to follow nearly neutrally buoyant tracer particles suspended in such flow. Typical particle trajectories are shown in figure 3. Particles within a vortex remain trapped for very long time (*stick*). Particles in the azimuthal jet experience prolonged *flights* around the circumference of the tank. Because the vortex pattern is not perfectly stationary particles alternate, apparently randomly, between flying in jets and sticking in vortices.

One can change the pattern of jets and vortices by altering the diameters of the circular barriers which confine the flow. Thus it is possible to create a flow with two oppositely directed jets separated by a vortex chain. In this case the dispersion process is more symmetric than in figure 4 because the flights go in both directions around the tank.

During a flight the angular displacement is proportional to the time

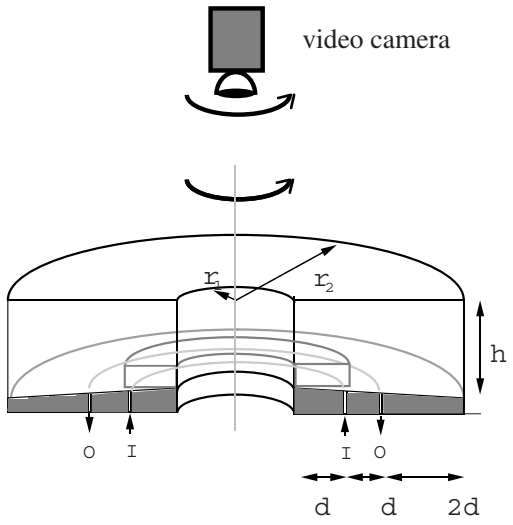


Figure 1: A sketch of the rotating annulus; the rotation rate is about 1Hz. Flow is forced by pumping water in through the ring of holes marked by I and withdrawing the same volume through the other ring marked O. As a consequence of the strong Coriolis forced acting on the radial flow between these concentric rings there is an azimuthal flow around the annulus. The experiment is viewed from above using a video camera. Figure courtesy of Eric Weeks.

Figure 2: Streaks formed by 100s trajectories of 12 particles reveal four vortices. Weeks et al. show that the motion of these coherent vortices is chaotic. That is, a velocity spectrum, obtained by measuring velocity with a hot film probe, is broad band. Figure courtesy of Eric Weeks.

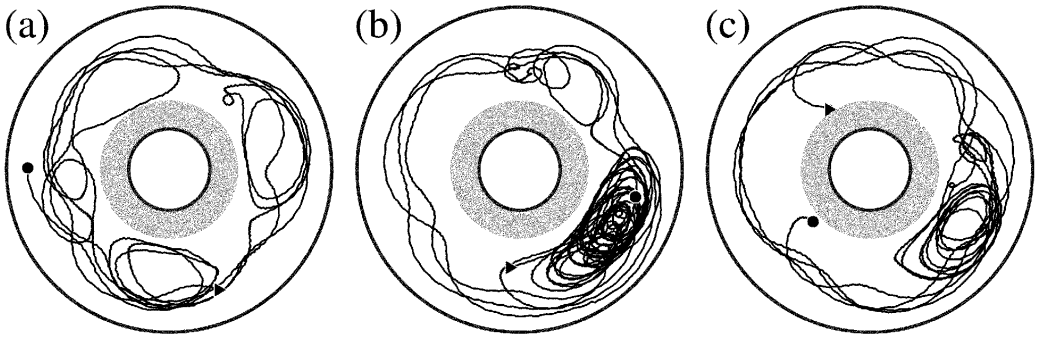


Figure 3: Trajectories of three tracer particles in the flow shown in figure 2. The beginning of each trajectory is indicated by a triangle and the end by with a circle. In (b) the particle spends most of its life trapped in a single vortex. However, this vortex wobbles erratically because the flow is chaotic. In parts (a) and (c) the particles experience several episodes of trapping within a vortex and flight around the tank in the jet. Figure courtesy of Eric Weeks.

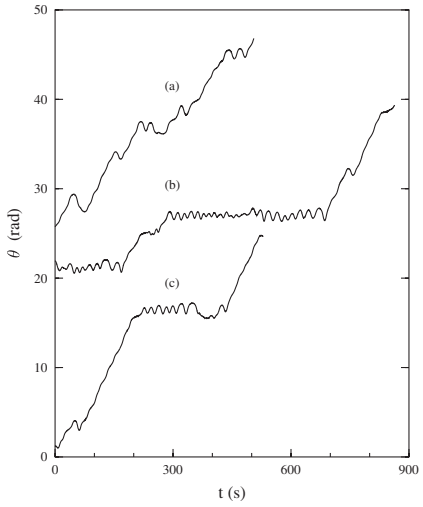


Figure 4: Angular displacement, $\theta(t)$ for the trajectories in figure 3. There is an obvious distinction between the flights and the sticking events. The small oscillations during the sticking events correspond to particle motion within a vortex. Figure courtesy of Eric Weeks.

elapsed since the flight began:

$$\Delta\theta \approx Ut. \tag{5}$$

The displacement, $\Delta\theta$, is essentially zero during a sticking event (see figure 4).

The experiments show that the dispersion of an ensemble of particles is superdiffusive. That is

$$\langle(\theta - \langle\theta\rangle)^2\rangle \sim t^\gamma \tag{6}$$

where $\gamma > 1$; typical values are $\gamma \approx 1.4$ to 1.7 depending on the experimental configuration. (It is also possible to observe normal diffusion, $\gamma = 1$, by strongly forcing the flow and breaking the azimuthal symmetry of the forcing.)

To characterize the motion Solomon et al. used sticking and flying PDFs:

$$\mathcal{P}_F(a)\mathrm{d}a = \text{ Probability that a flight has a duration} \in (a, a + \mathrm{d}a)\,. \tag{7}$$

Later in this lecture we will refer to $a$ as the "lifetime" of a particle in the flying or sticking state. We figuratively speak of a particle being born into the flying state and moving coherently for a lifetime $a$ so that the total angular displacement during the flight is $\Delta\theta = Ua$.

The PDF $\mathcal{P}_F$ is normalized by $\int_0^\infty \mathcal{P}_F(a)\mathrm{d}a = 1$ and

$$\tau_F = \int_0^\infty a\mathcal{P}_F(a)\,\mathrm{d}a = \text{average duration of a flight}\,. \tag{8}$$

The PDF of sticking times, $\mathcal{P}_S(a)$, and the average sticking time, $\tau_S$, are defined analogously.

Experiments show that as $a \to \infty$, $\mathcal{P}_F$ and $\mathcal{P}_S$ have algebraically decaying tails:

$$\mathcal{P}_F(a) \sim a^{-\mu_F}, \qquad \mathcal{P}_S(a) \sim a^{-\mu_S}, \tag{9}$$

with

$$2 < (\mu_F, \mu_S) < 3. \tag{10}$$

Because of this slow algebraic decay the variance of the lifetimes, defined by

$$\langle a^2\rangle_{F,S} \equiv \int_0^\infty a^2\mathcal{P}_{F,S}(a)\,\mathrm{d}a\,, \tag{11}$$

diverges.

The divergence of $\langle a^2 \rangle_F$ is significant because invoking Einstein's formula for the diffusivity

$$D = \frac{\langle (\Delta\theta)^2 \rangle}{\tau}\,, \tag{12}$$

and using $\Delta\theta = Ua$, we conclude that $D \propto \langle (\Delta\theta)^2 \rangle = U^2 \langle a^2 \rangle_F = \infty$. The divergence of $D$ is symptomatic of superdiffusion.

Notice that the denominator $\tau$ in (12) is related to the average flying and sticking times, $\tau_F$ and $\tau_S$, which are both finite. Thus, in the Texas experiments, we can say that anomalous diffusion occurs because the numerator of (12) is divergent. In other cases it is the denominator which causes trouble.

The Texas experiments show that anomalous diffusion occurs in realistic and geophysically relevant systems. Several theoretical questions suggest themselves. How do the algebraic tails of $\mathcal{P}_S$ and $\mathcal{P}_F$ arise, and can we make a microscopic models which exhibits this phenomenon? Can we relate the exponents $\gamma$, $\mu_F$ and $\mu_S$? (From section 4, the answer to the last question is $\gamma = 4 - \mu_F$.)

# 2 The telegraph model

The key issue raised by anomalous diffusion is decay of velocity correlations. Thus our goal is to formulate models for which we can explicitly calculate velocity statistics and understand the decay of correlations. Our first attempt is not very ambitious: we begin with the *telegraph model*, which is the simplest example of a continuous-time correlated random walk.

## 2.1 The Lagrangian formulation of the telegraph model

In a telegraph process the velocity of particle $n$, denoted by $u_n(t)$, can have only one of two possible values, $+U$ and $-U$. The velocity of each particle, $u_n(t)$, flips randomly back and forth between $\pm U$ with a transition probability $\alpha$ per time. This means that in a time $\mathrm{d}t$ a fraction $\alpha \mathrm{d}t$ of the ensemble switches velocity. Because the transition rate, $\alpha$, is constant we can say that a particle has no "memory" of when it first arrived in its present state. Thus this telegraph model is Markovian.

We refer to the prescription for constructing a telegraph process as *model A*. There is a variant, *model B*, discussed below.

With the prescription above, the velocity of a particle is a discontinuous function of time as shown in figure 5. The correlation function and the diffusivity are

$$\text{corr}(t) = U^2 e^{-2\alpha|t|}\,, \qquad D = \int_0^\infty \text{corr}(t)\,\mathrm{d}t = \frac{U^2}{2\alpha}\,, \qquad \text{(model A)}\,. \tag{13}$$

Notice that the $\text{corr}_{tt}$ is infinite at $t = 0$; this is because the acceleration is infinite at the discontinuities in figure 5.

To obtain (13), return to the definition of the correlation function

$$\text{corr}(t) = \frac{1}{N}\sum_{n=1}^{N} u_n(0)u_n(t), \tag{14}$$

where $N$ is the total number of particles in the ensemble. Suppose that at $t$ the sum on the right hand side has $P(t)$ positive terms, all equal to $U^2$, and $N - P(t)$ negative terms, all equal to $-U^2$. Thus

$$\text{corr}(t) = \frac{U^2}{N}[2P(t) - N]\,. \tag{15}$$

In a time $\mathrm{d}t$, $P\alpha\mathrm{d}t$ of the positive terms become negative and $(N - P)\alpha\mathrm{d}t$ of the negative terms become positive. Thus, at $t + \mathrm{d}t$,

$$P(t + \mathrm{d}t) = P(t)(1 - 2\alpha\mathrm{d}t) + N\alpha\mathrm{d}t\,, \tag{16}$$

and the analog of (15) is:

$$\text{corr}(t + \mathrm{d}t) = \frac{U^2}{N}[2P(t)(1 - 2\alpha\mathrm{d}t) + 2N\alpha\mathrm{d}t - N]\,. \tag{17}$$

Taking the limit $\mathrm{d}t \to 0$ in (17) gives $\text{corr}_t = -2\alpha\text{corr}$; the solution of this differential equation is (13).

An alternative telegraph process (model B) is constructed by imagining that at random instants each particle flips at coin. The flipping rate is $\alpha$ so that in a time $\mathrm{d}t$, there are $N\alpha\mathrm{d}t$ coin flips. After each flip, the velocity is $+U$ if there is a head and $-U$ if a tail. With this prescription, a particle will change direction on average once out of every two tosses. On the other tosses

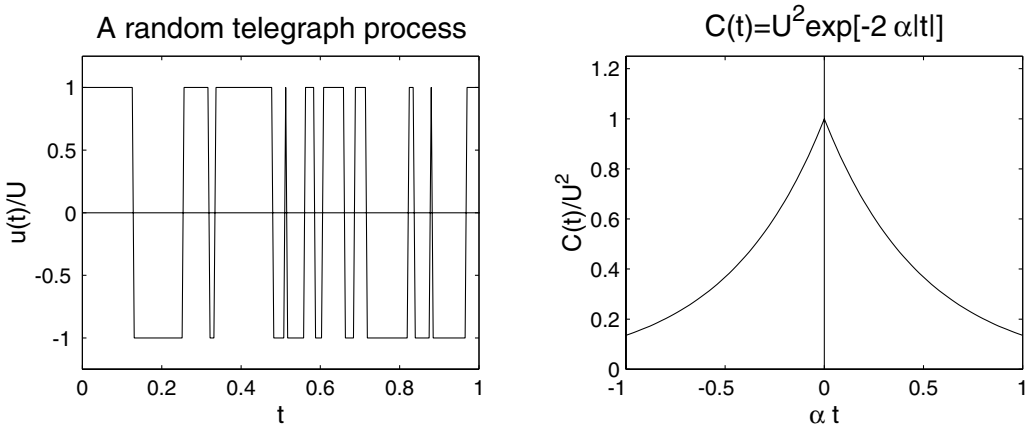


Figure 5: An example of a telegraph time series, and the telegraph correlation function.

the particle continues in the same direction and the result is as if nothing happened. Thus with model B we simply replace $\alpha$ by $\alpha/2$ in our earlier calculations and consequently the correlation function and diffusivity are

$$\text{corr}(t) = U^2 e^{-\alpha|t|}, \qquad D = \int_0^\infty \text{corr}(t)\,\mathrm{d}t = \frac{U^2}{\alpha}, \qquad \text{(model B)}. \tag{18}$$

The difference between model A and model B is trivial. However the distinction between the two cases will plague us later.

If we are searching for a model of anomalous diffusion then the telegraph model is a disappointment: the exponentially decaying correlation function ensures that $D$ is finite and that the displacement variance ultimately grows diffusively. We continue our investigation of the telegraph model in order to better understand "ultimately" and because in section 4 the telegraph model is used as the foundation of more elaborate models which do show anomalous diffusion.

## 2.2 The Eulerian formulation of the telegraph model

Now we ignore the Lagrangian information contained in the correlation function (14) and instead we give an Eulerian formulation of the telegraph process. Let $R(x,t)$ denote the density (particles/length) of particles moving to the right with velocity $+U$ and $L(x,t)$ denote the density of left-moving

particles with velocity $-U$. The coupled conservations laws are

$$R_t + UR_x = \alpha(L - R), \qquad L_t - UL_x = \alpha(R - L). \tag{19}$$

These equations should be self-evident...

We can put (19) into a revealing alternative form by defining the total concentration, $C(x,t)$, and the flux, $F(x,t)$, as

$$C \equiv R + L\,, \qquad F \equiv U(R - L)\,. \tag{20}$$

In terms of these new variables the model is

$$C_t + F_x = 0\,, \qquad F_t + 2\alpha F = -U^2 C_x\,. \tag{21}$$

The first equation is conservation of particles and the second equation is the flux-gradient relation.

Notice that in (21) Fick's law does not apply — the flux $F$ is not instantaneously related to the gradient $C_x$. Equation (21b), which might be called Cattaneo's law (see the 1989 review by Joseph and Preziosi), can be solved as a first-order differential equation for $F(x,t)$. Thus, the flux at $x$ is expressed as weighted integral over the past history of the gradient at $x$:

$$F(x,t) = -U^2 \int_{-\infty}^{t} e^{-2\alpha(t-t')} C_x(x,t')\,\mathrm{d}t'\,. \tag{22}$$

The flux has a "fading memory" of the gradient and the exponential in (22) is the fading factor which strongly weights the most recent values of the gradient.

Next, if we eliminate $F$ from (21), we obtain

$$C_{tt} + 2\alpha C_t - U^2 C_{xx} = 0\,. \tag{23}$$

This is the telegraph equation; the diffusion equation is obtained only as an approximation which applies to the low frequency and wavenumber components of $C(x,t)$. On these large and slowly evolving scales one can neglect the term $C_{tt}$ in (23) and so obtain the approximation

$$C_t \approx DC_{xx}\,, \qquad D = \frac{U^2}{2\alpha}\,. \tag{24}$$

The diffusivity $D$ in (24) was anticipated in (13).

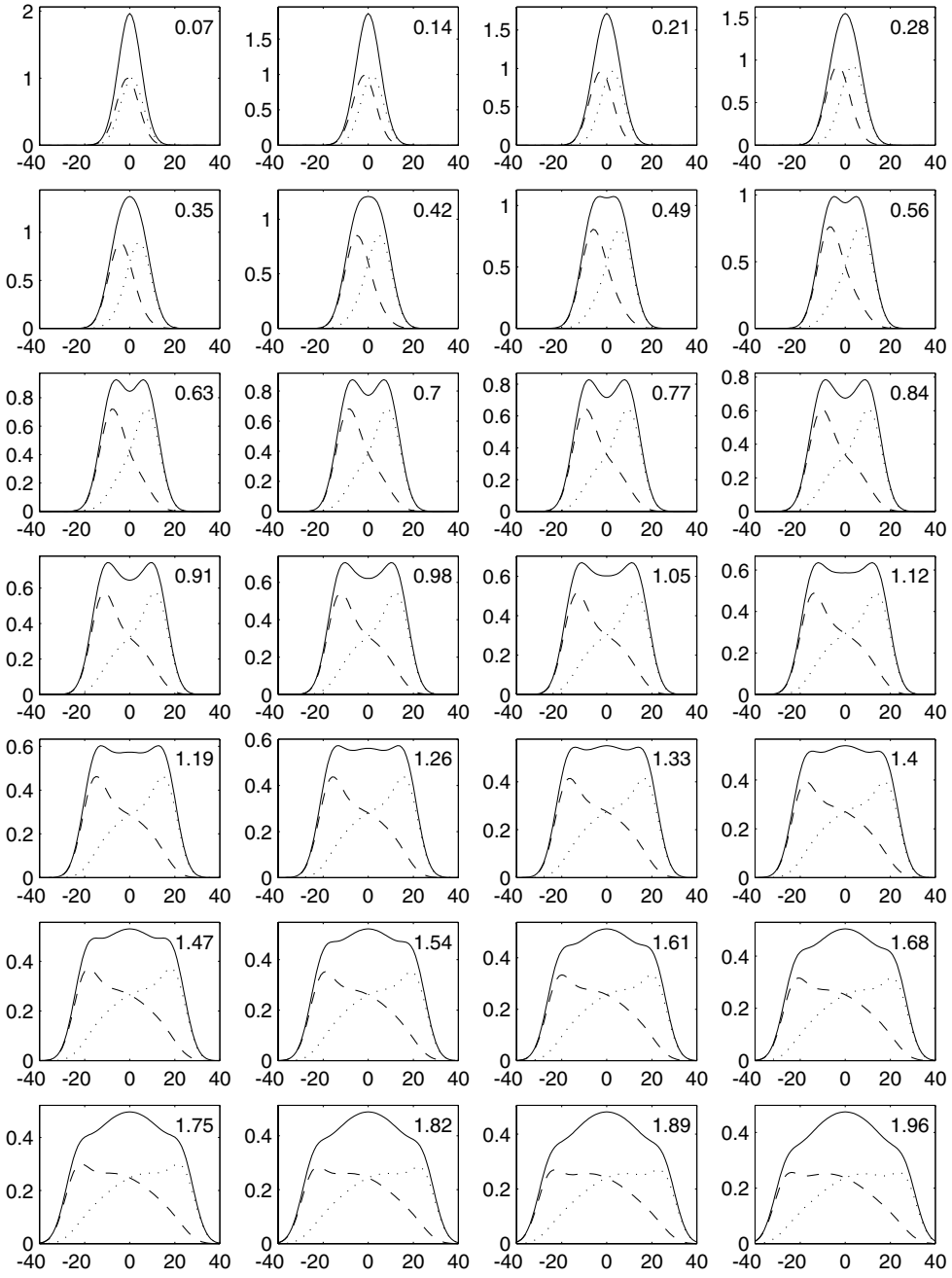


Figure 6: Solution of the telegraph equation. $\alpha t$ is in the top corner of the panel. At $t = 0$, $R = L = \exp(-x^2/50)$. The solid curve is $C = R + L$, and $R$ and $L$ are shown as dotted and dashed curves.

Figure 6 shows a numerical solution of (23) starting with an initial condition of the form

$$R(x,0) = L(x,0) = e^{-\mu^2 x^2}. \tag{25}$$

At small times the density $C$ develops a double peaked structure as the left and right going populations separate. This behaviour is transient, and at longer times the central part of the concentration relaxes to the well-known Gaussian solution of the diffusion equation.

According to (23) the disturbance travels at a finite speed: these are the "heat waves" discussed by Joseph and Preziosi (1989), and also evident in figure 6. The approximate diffusion equation (24) makes the unrealistic prediction that disturbances are propagated at infinite speed. This unphysical consequence of the diffusion equation motivated Cattaneo to propose (21b) as an alternative to Fick's law.

These considerations shows that one cannot blithely assert the validity of the diffusion equation (24) as an exact description of dispersion. The diffusion equation applies only as an approximate description of low frequencies and long wavelengths.

## 2.3 Discretization of the telegraph model

This section is a digression. Read on if you want to learn how to solve the telegraph equation using a simple numerical scheme. (This is how I drew figure 6.)

We reformulate the telegraph model in terms of discrete variables: divide the $x$-axis is divided into segments of length $\delta x$ separated by "scattering sites" at $x_n = n\delta x$. Time is also discretized in units of $\delta t$ so that $t = T\delta t$ where $T$ is an integer $T = 0, 1, 2 \cdots$ The walkers move along the $x$–axis with a velocity that is either $+\delta x/\delta t$ or $-\delta x/\delta t$. In terms of the continuous model in (19)

$$U = \frac{\delta x}{\delta t}\,. \tag{26}$$

When a walker reaches the scattering site at $x_n = n\delta x$ he is "backwards scattered" or reflected with probability $b$ and "forward scattered" or transmitted with probability $1 - b$. Because the probability of a change in direction, $b$, is the same for left as for right moving walkers there is no mean velocity along the line.

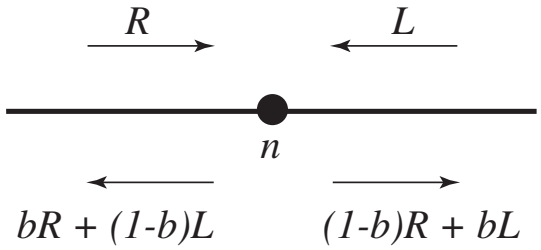


Figure 7: A steady state with constant flux, $f = U(1-b)(R-L)$, passing through site $n$.

Let $R_n(T)\delta x$ be the number of right walkers in the segment $n$, $n\delta x < x < (n+1)\delta x$. The number of left walkers, $L_n(T)\delta x$, is defined analogously. $R_n$ and $L_n$ are the discrete analogs of the continuous densities used in (19).

With these rules and definitions, the discrete evolution equations for the ensemble are

$$R_n(T) = (1-b)R_{n-1}(T-1) + bL_n(T-1)\,, \tag{27}$$

$$L_n(T) = (1-b)L_{n+1}(T-1) + bR_n(T-1)\,. \tag{28}$$

For instance, in the first equation above, the number of right movers in segment $n$ is equal to the number in segment $n-1$ at the previous time that successfully passed through scattering site $n$, plus the number of left movers previously in segment $n$ that were reflected at this same site. Figure 6 shows the result of iterating the discrete system above.

One exact solution of the difference equations above is

$$R_n = L_n = L_{n+1} = R_{n+1} = \cdots \tag{29}$$

This solution is steady: $R_n(T) = R_n(T-1)$. In fact, (29) is the discrete analog of the *equilibrium* solution of the diffusion equation. The distribution of walkers is spatially uniform with equal numbers going left and right in each interval and there are no concentration gradients. An individual walker is moving to and fro, but the ensemble is in steady state.

Next, we consider the *constant-flux* solution. In figure 7, $R$ right walkers impinge on site $n$ from the left and $L$ left walkers impinge on $n$ from the right. In steady state it must be that on the left of $n$ there are $bR + (1-b)L$ left walkers moving away, while to the right there are $bL + (1-b)R$ right

walkers moving away. Thus the flux to the right of the site is

$$f = U\left[(1-b)\,R + bL\right] - UL = \frac{\delta x}{\delta t}(1-b)(R-L)\,, \tag{30}$$

where we have used $U = \delta x/\delta t$. Because there is a steady state, calculating the flux to the left of the site gives exactly the same result and so there is a nondivergent flux of walkers along the line.

Next, we can calculate the concentration difference across the site in figure 7. To the right of the site the total density of walkers is

$$c^+ = L + bL + (1-b)R\,, \tag{31}$$

while on the left the density is

$$c^- = R + bR + (1-b)L. \tag{32}$$

Combining (31) and (32) we have for the concentration jump across the site

$$\delta c = c^+ - c^- = 2b(L-R) \tag{33}$$

Thus, using (30), the flux-gradient relation in steady state is

$$f = -D\,\frac{\delta c}{\delta x}\,, \qquad D = \frac{(1-b)}{2b}\frac{(\delta x)^2}{\delta t}\,. \tag{34}$$

Does it seem obvious to you that the diffusivity should diverge as $b \to 0$? If you think of the diffusivity as the area under the correlation functions then this divergence should be intuitive. It is an instructive exercise to obtain $D$ in (34b) using Taylor's formula. (Hint: consider $N \gg 1$ right walkers which initially set out together. At $t = T\delta t$, after $T$ encounters with scattering sites, how many of these walkers have changed direction an even number of times, and how many odd?)

Comparing the equation above with our earlier expression for the diffusivity, $D$ in (13) and (24), we conclude that

$$\alpha\delta t = \frac{b}{1-b}\,. \tag{35}$$

Thus, with (26) and (35), we can express the parameters of the discrete model, $(\delta x, \delta t, b)$, in terms of the parameters characterizing the continuous model, $U$ and $\alpha$.

# 3 Age-stratified populations

The telegraph model from section 2 is *Markovian*. This means that each particle has a constant probability per unit time, $\alpha$, of switching direction. Thus, no matter how long a particle has been moving to the right (say), its probability of switching direction in the next $\mathrm{d}t$ is always $\alpha \mathrm{d}t$. Consequently an exponentially decreasing number of particles move coherently for long intervals and the telegraph model in (19) does not exhibit anomalous diffusion.

A satisfactory description of anomalous diffusion demands a non-Markovian model in which particles have some memory of their past motion. To obtain superdiffusion it is necessary that a right-moving particle is less and less likely to change direction as it spends more and more time moving right[1].

Such memory effects are implicit in the models discussed by Weeks et al (1996), and in several of the articles in the conference proceedings edited by Schlesinger, Zaslavsky & Frisch (1994). The stochastic models discussed in Schlesinger et al. draw heavily on statistical physics. In this lecture we are going to develop the theory from scratch using a formalism which is accessible to people whose background is in fluid mechanics. The climb begins with an excursion into the theory of age-stratified populations.

Consider a population of items with a finite lifetimes and a death rate which depends on age, $a$. For example, light bulbs in a large building, or the population of the United States. At time $t$ the age structure of the population is characterized by a density function for which $f(a,t)\mathrm{d}a$ is the number of items whose age is between $a$ and $a+\mathrm{d}a$. In terms of $f$, the total number of items in the population, $N(t)$, and the average age, $\bar{a}(t)$, are given by

$$N(t) = \int_0^\infty f(a,t)\,\mathrm{d}a, \qquad \bar{a}(t) \equiv N^{-1}\int_0^\infty a f(a,t)\,\mathrm{d}a. \tag{36}$$

The density function evolves according to

$$f_t + f_a + \alpha f = 0, \tag{37}$$

[1] A popular metaphor for the Markovian case is radioactive decay: a molecule has a constant probability per unit time of decaying. As a metaphor for the non-Markovian case, imagine entering an enormous maze and then trying to find your way back to the entrance. The longer one has wandered, the less the chance of stumbling on the exit in the next $\mathrm{d}t$.

where $\alpha(a)$ is the death-rate. The term $f_a$ in (37) says that the population translates along the age-axis at a rate one year every year. To completely specify the problem we must supply an initial condition, and also a boundary condition at $a = 0$. The boundary condition at $a = 0$ has an obvious interpretation:

$$f(0,t) = \text{the birth (or replacement) rate.} \tag{38}$$

In the case of a population of people, the boundary condition above is a flux of babies into the system.

The Markovian limit is the special case in which $\alpha$ is independent of $a$. This model of $\alpha$ is unrealistic for both light-bulbs and people, though it might apply to a population of radioactive molecules. The Markovian case is very simple because one can integrate (37) over $a$ and obtain a closed equation for $N(t)$:

$$N_t + \alpha N = f(0,t)\,. \tag{39}$$

Thus if $\alpha$ is constant and we need only the total number of functional items at $t$ then we do not need to solve partial differential equations and deal with the age structure of the population.

## 3.1 The steady-state solution

As a first illustrative example, suppose that the replacement rate is adjusted so that $N$ is constant. (Janitors replace light bulbs as soon as they burn-out.) In this case the equilibrium solution of (37) is

$$f(a) = N\tau^{-1}\Psi(a), \tag{40}$$

where

$$\Psi(a) \equiv \exp\left(-\int_0^a \alpha(a')\,\mathrm{d}a'\right), \qquad \tau \equiv \int_0^\infty \Psi(a)\,\mathrm{d}a. \tag{41}$$

The function $\Psi$, and its integral $\tau$, will occur frequently in the sequel. Notice that the replacement rate is $f(0) = N/\tau$ and this suggests that $\tau$ should be the average lifetime of an item. On the other hand, $\tau$ will not usually be equal to $\bar{a}$ in (36). I suggest brooding on this "paradox" and, as an exercise, see if you can resolve this confusion to your satisfaction by the end of this section.

In (41) we assume that the death rate $\alpha(a)$ is such that as $a \to \infty$, $\Psi(a) \to 0$ fast enough to ensure that $\tau$ is finite. For instance, if $\alpha$ is constant (this is the Markovian case) then $\Psi(a) = \exp(-\alpha a)$ and $\tau = \bar{a} = 1/\alpha$.

If the death rate $\alpha$ decreases with age then the average liftetime $\tau$ might not be finite. For example, consider the specific model

$$\alpha = \frac{\nu}{\theta + a}, \qquad \Rightarrow \qquad \Psi(a) = \left(\frac{\theta}{\theta + a}\right)^{\nu}. \tag{42}$$

Provided that $\nu > 1$ then the integral of $\Psi(a)$ converges and $\tau = \theta/(\nu - 1)$.

If $\nu < 1$ then $\tau = \infty$ and there is no steady solution. To understand this curious result we must solve an initial value problem (see appendix 5). Here we just remark that if $\nu < 1$ then the average lifetime of a bulb is infinite. Detailed solution of the initial value problem in appendix 5 shows that in this case the replacement rate is $f(0,t) \propto t^{\nu-1}$. That is, the total number of new bulbs which have been installed at time $t$ grows like $t^{\nu} \ll t$. The hypothetical manufacturer of lightbulbs with $\nu < 1$ is threatened with bankruptcy: sales decrease with time, even though every bulb eventually fails.

## 3.2 A cohort of babies

Imagine a cohort of babies leaving the maternity ward together, or a box of new lightbulbs shipped fresh from the factory. These items will function for varying amounts of time, and so we can speak of the PDF of lifetimes. We denote this PDF by $\mathcal{P}(a)$, and our goal is to relate $\mathcal{P}(a)$ to the death rate $\alpha(a)$.

Consider a group of $N$ items which all start with $a = 0$ at $t = 0$. What fraction of this cohort survives at $t > 0$? The surviving fraction is also the fraction of lifetimes longer than $t$ and so

$$\text{surviving fraction at } t \equiv \Psi(t) = \int_t^{\infty} \mathcal{P}(a)\, \mathrm{d}a. \tag{43}$$

To calculate the surviving fraction, we solve (37) with the initial and boundary conditions

$$f(a,0) = N\delta(a), \qquad f(0,t) = 0. \tag{44}$$

The solution of (37) and (44) is

$$f(a,t) = N\Psi(t)\delta(a - t)\,, \tag{45}$$

where $\Psi$ is defined in (41). Thus $\Psi(t)$ is the fraction of the cohort which is still alive at time $t$; we refer to $\Psi$ as the *s*urvival function.

It now follows from (43) that the PDF of lifetimes of new items is

$$\mathcal{P}(a) = -\Psi_a = \alpha\Psi. \tag{46}$$

The average lifetime, $\tau$, is given by the equivalent expressions:

$$\tau = \int_0^\infty a\mathcal{P}(a)\,\mathrm{d}a = -\int_0^\infty a\Psi_a\,\mathrm{d}a = \int_0^\infty \Psi(a)\,\mathrm{d}a. \tag{47}$$

Thus, as was suggested in the discussion following (41), to keep a population in equilibrium the replacement rate is equal to the size of the population, $N$, divided by the average lifetime of *new* items, $\tau$.

## 3.3 Extinction of a population

As a final example, suppose that at $t = 0$ we have the steady-state lightbulb population in (40). If the janitors then go on strike, so that bulbs burn out without replacement, then how many bulbs are still operating at $t > 0$? In this example we must solve (37) with the initial and boundary conditions that

$$f(a,0) = N\tau^{-1}\Psi(a), \qquad f(0,t) = 0\,. \tag{48}$$

The solution is

$$f(a,t) = H(a-t)N\tau^{-1}\Psi(a)\,, \tag{49}$$

where $H(a-t)$ is the step function. Thus the fraction of surviving bulbs at $t$ is

$$\Theta(t) = \tau^{-1}\int_t^\infty \Psi(a)\,\mathrm{d}a = \tau^{-1}\int_t^\infty (a-t)\mathcal{P}(a)\,\mathrm{d}a. \tag{50}$$

Using the specific model of $\alpha$ in (42), the surviving fraction is

$$\Theta(t) = (1+\theta^{-1}t)^{1-\nu}. \tag{51}$$

$\Theta(t)$ is the most slowly decaying function we have seen so far: as $t \to \infty$, $\Theta(t) \gg \Psi(t) \gg \mathcal{P}(t)$. This model may be relevant to the very slow extinction of professors once the supply of graduate students is cut-off.

Comparing the results in sections 3.1 and 3.2, we see that the steady state population in section 3.1 contains more long-lived items than are in a cohort of new items section 3.2. This means that the average lifetime of the light bulbs currently operating in the Empire State building is longer than the average lifetime of bulbs shipped from the factory. The reason is obvious: items with brief lifetimes fail quickly, and will likely be replaced with items whose lifetime is closer to the mean. Thus, fragile individuals are underrepresented in an operational population.

# 4 The generalized telegraph model

## 4.1 Formulation

Using the machinery from the previous section we now construct a generalization of the telegraph model which exhibits anomalous diffusion. In this generalization particles switch randomly between moving with $u(t) = +U$, $u(t) = 0$ and $u(t) = -U$. The transition probabilities between these states are functions of the time since the last transition. In other words, each particle carries an "age", $a$, which is the time elapsed since the particle transitioned into its present state. We denote the density of right moving particles at $(x, t)$, with age $a$, by $\mathcal{R}(a, x, t)$. For left-moving particles the density is $\mathcal{L}(a, t, x)$, and for the stationary particles the density is $\mathcal{S}(a, x, t)$. We refer to the left and right–movers collectively as "flying particles" while the stationary particles are "stickers".

The flying particles satisfy the conservational laws

$$\mathcal{R}_t + \mathcal{R}_a + U\mathcal{R}_x + \alpha_F \mathcal{R} = 0, \quad \mathcal{L}_t + \mathcal{L}_a - U\mathcal{L}_x + \alpha_F \mathcal{L} = 0\,, \tag{52}$$

while the sticking particles have

$$\mathcal{S}_t + \mathcal{S}_a + \alpha_S \mathcal{S} = 0\,. \tag{53}$$

The death rates of flying and sticking particles, $\alpha_F$ and $\alpha_S$ respectively, are functions of age $a$; it is through this device that particles have a memory of their previous history. The price we pay for this nonMarkovian memory is that there are now three independent variables, $(a, t, x)$.

Stationary particles are born when left and right-moving particles die. And, conversely, when a stationary particle dies it is reborn as either a left

moving particle or a right moving particle with equal probability. Notice that in order for a right-moving particle to become a left-moving particle it must pass through the intermediate state with $u = 0$. These karmic rules are enforced by boundary conditions at $a = 0$:

$$\mathcal{L}(0,t,x) = \mathcal{R}(0,t,x) = \frac{1}{2}\int_0^\infty \alpha_S(a)\mathcal{S}(a,t,x)\,\mathrm{d}a\,, \tag{54}$$

and

$$\mathcal{S}(0,t,x) = \int_0^\infty \alpha_F(a)\left[\mathcal{L}(a,t,x) + \mathcal{R}(a,t,x)\right]\,\mathrm{d}a\,. \tag{55}$$

Trajectories of particles moving with this generalized telegraph process are shown in figure 8.

The model we have formulated here is a generalization of the telegraph model in two ways. First, there are three states: left, right and stationary. This minor embellishment is motivated by the Texas experiments in which trapping in a vortex corresponds to the stationary particles. The nontrivial generalization is the introduction of the age variable used to capture memory effects. As an exercise, the student can show that if $\alpha_F$ and $\alpha_S$ are independent of $a$ then one can easily integrate over $a$ and reduce (52) through (55) to a three-state telegraph model. (This exercise shows how the boundary condition at $a = 0$ works.) As a sequel to this exercise, discuss $\alpha_S \to \infty$ and show that in this limit one obtains effectively a two-state telegraph model. Are you surprised that the diffusivity is given by (18)? That is, why do we recover model B, rather than model A, when the sojourns in the intermediate state $u = 0$ are very brief?

In order to model slowly fading velocity correlations and anomalous diffusion we use

$$\alpha_F(a) = \frac{\nu_F}{\theta_F + a}\,, \qquad \alpha_S(a) = \frac{\nu_S}{\theta_S + a}\,. \tag{56}$$

With the form above, the transition rates decrease as particles age. Numerical simulations of the three-state model using the transition rates in (56) show that many particles move in the same direction for a long time (see figure 9).

The main point of (56) is that if $a \gg 1$ then the transition rates $\alpha_F$ and $\alpha_S$ are proportional to $a^{-1}$. This inverse dependence on age ensures that the flying and sticking PDFs, $\mathcal{P}_F$ and $\mathcal{P}_S$ in (7), decay algebraically.

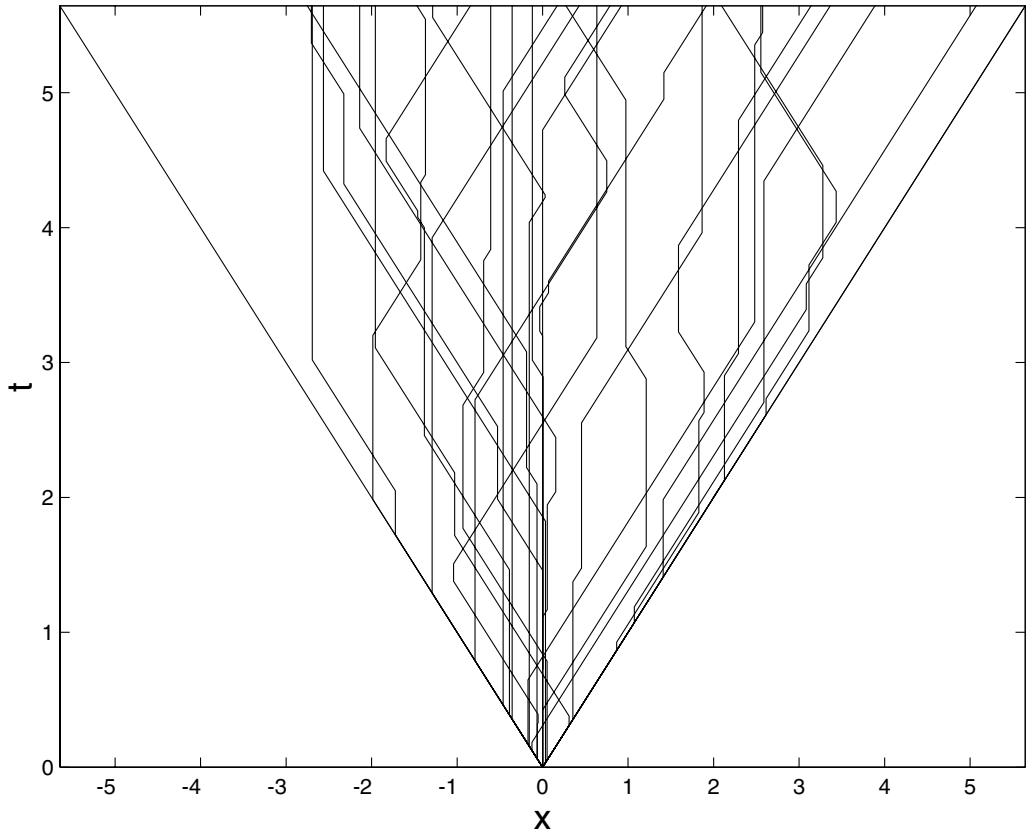


Figure 8: Trajectories of particles in the generalized telegraph random process. All particles are released from $x = 0$.

Thus (56) incorporates important experimental information into the model[2]. One can make a dimensional argument in support of (56): $\alpha_F$ and $\alpha_S$ have the dimensions of inverse time. If the only time-scale relevant for long-lived particles is the particle age, $a$, then it follows that $\alpha_F$ and $\alpha_S$ are inversely proportional to $a$. We now show that the parameters $\nu_F$ and $\nu_S$ are easily related to the experimentally measured exponents $\mu_F$ and $\mu_S$ in (9).

[2]As far as scaling exponents are concerned, only the $a \gg 1$ structure of $\alpha_F$ and $\alpha_S$ matter. We use the specific functional form in (56) for simplicity.

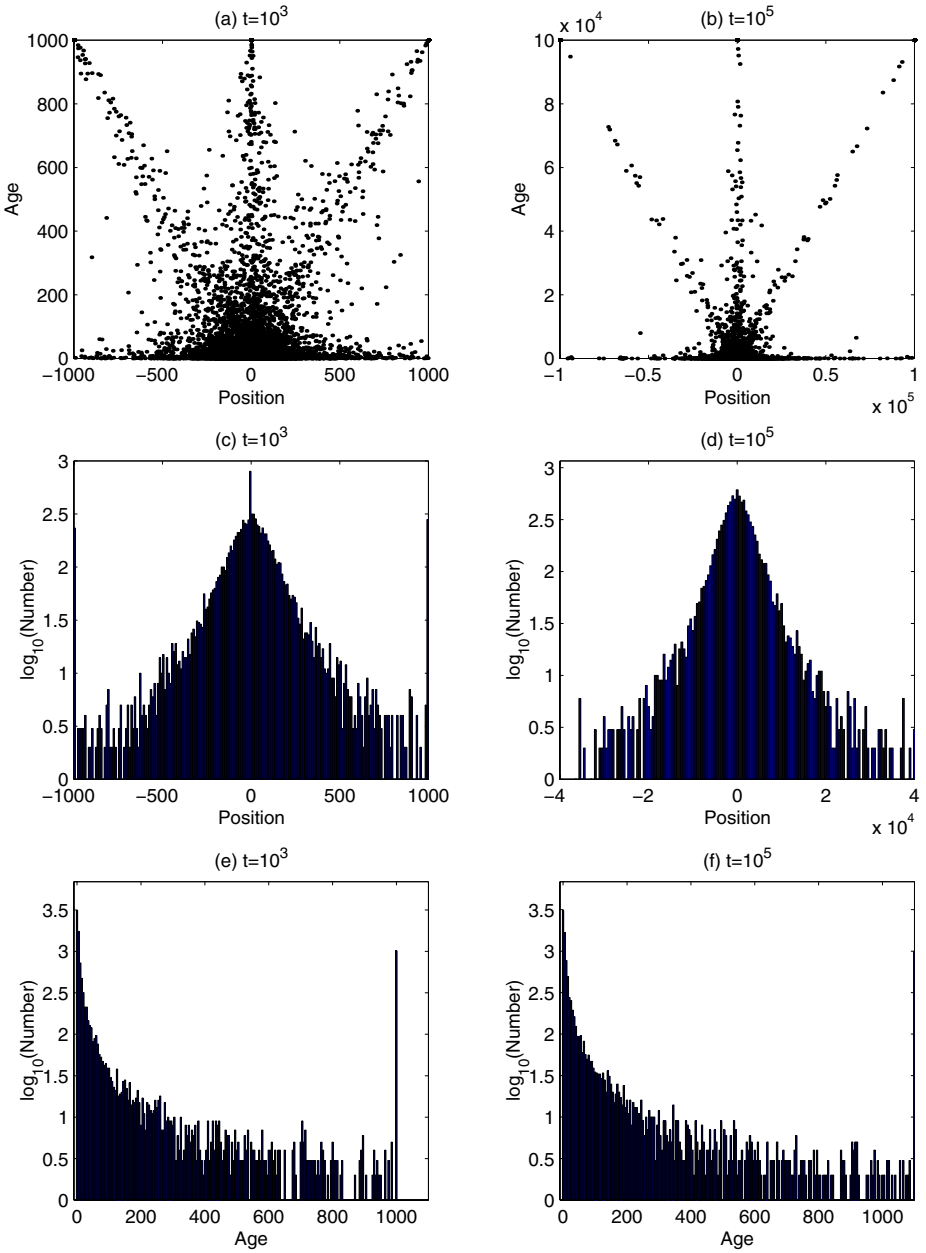


Figure 9: A simulation with $N = 10^4$ particles; $\alpha_F(a) = \alpha_S(a) \sim 1.35/a$. Upper panels: PDFs as a function of age and position show that there are many particles that either stick or move at a constant velocity for nearly the whole simualtion. Center panels: PDFs of the position of particles develop tails larger than Gaussians as time goes on. Lower panels: PDFs of the age of particles have a spike at large times, because there is a fraction of particles that never die.

## 4.2 The equilibrium solution

The system (52) through (55) has a solution which is homogeneous ($\partial_x = 0$) and steady ($\partial_t = 0$). This equilibrium solution is

$$\mathcal{R}(a,x,t) = \mathcal{L}(a,t,x) = r\Psi_F(a), \qquad \mathcal{S}(a,t,x) = 2r\Psi_S(a) \tag{57}$$

where $\Psi_{F,S}(a)$ is

$$\Psi_{F,S}(a) \equiv \exp\left(-\int_0^a \alpha_{F,S}(a')\,\mathrm{d}a'\right). \tag{58}$$

The constant $r$ in (57) is the transition rate between the different states; $r$ is determined by the normalization condition:

$$N = 2r\left(\tau_S + \tau_F\right), \qquad \tau_{F,S} \equiv \int_0^\infty \Psi_{F,S}(a)\,\mathrm{d}a\,. \tag{59}$$

We can use the results from section 3 to interpret $\tau_F$ and $\tau_S$ as the average lifetimes in the flying and sticking states respectively. Using (46), the PDF of lifetimes in those states is given by

$$\mathcal{P}_{F,S} = \alpha_{F,S}\Psi_{F,S}\,. \tag{60}$$

Using the expression in (56) for $\alpha_{F,S}$, we see that as $a \to \infty$, the survival functions decay algebraically with $\Psi_{F,S} \sim a^{-\nu_{F,S}}$, and so $\mathcal{P}_{F,S} \sim a^{-\nu_{F,S}-1}$. It follows that the exponents $\mu_F$ and $\mu_S$ defined in (9) are related to $\nu_F$ and $\nu_S$ by

$$\mu_{F,S} = \nu_{F,S} + 1\,. \tag{61}$$

We can summarize our arguments to this point by observing that the experiments provide the flying velocity, $U$, the average lifetime in the flying and sticking states, $\tau_{F,S}$, and the exponents $\mu_{F,S}$. These five experimental data determine the five parameters in the generalized telegraph model, namely $(U, \nu_{F,S}, \theta_{F,S})$.

## 4.3 Formulation of the initial value problem

Now that we have determined the model parameters using experimental constraints it is time to do some mathematics and use the model to predict the

exponent $\gamma$ in (6). The simplest intial value problem we can consider is (52) through (55) with

$$[\mathcal{R}(a,0,x),\mathcal{S}(a,0,x),\mathcal{L}(a,0,x)] = r\,[\Psi_F(a), 2\Psi_S(a), \Psi_F(a)]\,\delta(x). \tag{62}$$

The constant $r$ is given in (57). Thus, the initial population has an equilibrium distribution of ages and is released at $x = 0$. Because of the symmetry between left and right moving particles

$$\mathcal{R}(a,t,x) = \mathcal{L}(a,t,-x), \qquad \mathcal{S}(a,t,x) = \mathcal{S}(a,t,-x). \tag{63}$$

Equation (63) greatly simplifies subsequent algebra.

One technical point (which I confess confuses me) is using the equilibrium age distribution as the initial condition in (62). This choice leads to simple calculations below. And perhaps the gross details of the dispersion process, such the exponent $\gamma$, are independent of the initial distribution of ages? As an excercise I suggest solving the initial value problem using other initial conditions e.g., $\mathcal{R}(a,0,x) = \delta(a)\delta(t)$ etcetera. Are there any significant differences in the $t \to \infty$ structure of the solution?

Our strategy will be to obtain a closed hierarchy of spatial moments by multiplying the conservation laws (52) and (53) by $x^n$ and integrating over $x$. It is possible to solve the first few members of the hierarchy and show that if $\alpha_{F,S}$ and has the form in (56) with $1 < \nu < 2$ then as $t \to \infty$

$$\langle x^2\rangle = \int_0^\infty \int_{-\infty}^\infty x^2\,[\mathcal{R}(a,t,x) + \mathcal{S}(a,t,x) + \mathcal{L}(a,t,x)]\;\mathrm{d}x\mathrm{d}a \propto t^{3-\nu_F}\,. \tag{64}$$

Before entering this calculation, we give a simple argument which suggests how the anomalous exponent $3 - \nu_F > 1$ arises in (64).

The variance $\langle x^2\rangle$ in (64) can alternatively be written as

$$\langle x^2\rangle = \frac{1}{N}\sum_{n=1}^{N} x_n^2. \tag{65}$$

At time $t > 0$ some of the $N$ particles will have moved coherently with unchanging velocity (either $+U$ or $-U$) ever since $t = 0$; half of these particles will be at $x = Ut$ and the other half at $x = -Ut$. These "coherent particles" each contribute a term $U^2t^2$ to the sum on the right hand side of (65). The number of coherent flying particles is just $\Theta(t)N$ where $\Theta(t)$ is given by

(51) with $\nu$ replaced by $\nu_F$. Thus, because every term in the sum in (65) is positive, one has

$$\langle x^2 \rangle > \Theta(t) U^2 t^2 \sim U^2 \theta_F^{\nu-1} t^{3-\nu_F} \tag{66}$$

The inequality (66) has teeth only if $3 - \nu_F > 1$: then we learn that the coherent particles alone produce a superdiffusive contribution to the variance.

The argument above may suggest to you that superdiffusion is due solely to the few extreme particles which move without changes in direction. This is an overstatement: the lower bound in (66) is generously less than the exact result for $\langle x^2 \rangle$ which we obtain in the next section. Thus "nearly-coherent" particles, meaning particles which change direction only once or twice, also make a large contribution to the sum in (65). This is an essential point, because in their analysis of the experiments Solomon et al. discarded all coherent particles from the data set[3]. Thus the exponent measured by Solomon et al reflects only the contribution of nearly coherent particles.

## 4.4 Solution of the initial value problem

This is a dry section which contains the details of the analytic calculation of $\langle x^2 \rangle$. The main point of interest here is that a lot of the algebra can be avoided by proving (75) below. (I suggest this as an exercise.)

The spatial moments are defined by

$$\left[\mathcal{R}_n\left(a,t\right), S_n(a,t), \mathcal{L}_n\left(a,t\right)\right] \equiv \int_{-\infty}^{\infty} x^n \left[\mathcal{R}(a,t,x), \mathcal{S}(a,t,x)\mathcal{L}(a,t,x)\right] \mathrm{d}x, \tag{67}$$

Because of the symmetry in (63)

$$\mathcal{R}_n(a,t) = (-1)^n \mathcal{L}_n(a,t), \qquad \mathcal{S}_n(a,t) = 0 \text{ if } n \text{ is odd.} \tag{68}$$

The result above allows us to work exclusively with $\mathcal{R}_n$ and $\mathcal{S}_n$ while retaining full information about the distribution. Using the symmetry, the variance can be written as

$$\langle x^2 \rangle = \int_0^{\infty} 2R_2 + S_2 \, \mathrm{d}a \, . \tag{69}$$

[3]This drastic procedure is necessary because some fraction of the experime ntal particles are in integrable regions and will fly forever. Retaining all these particles will ultimately lead to the trival ballistic exponent $\gamma = 2$.

The zeroth moment of (52) through (55), with the initial condition in (62) is

$$[\mathcal{R}_0(a,t), \mathcal{S}_0(a,t), \mathcal{L}_0(a,t)] = r\left[\Psi_F(a), 2\Psi_S(a), \Psi_F(a)\right]. \tag{70}$$

That is, the zeroth moment is just the equilibrium solution. (This is why using the equilibrium age distribution as the initial condition is so convenient.)

Using (68), the first spatial moment is $\mathcal{S}_1 = 0$, $\mathcal{L}_1(a,t) = -\mathcal{R}_1(a,t)$ and

$$\mathcal{R}_{1t} + \mathcal{R}_{1a} + \alpha_F \mathcal{R}_1 = Ur\Psi_F, \qquad \mathcal{R}_1(0,t) = 0, \qquad \mathcal{R}_1(a,0) = 0. \tag{71}$$

The solution of the initial value problem (71) is

$$\mathcal{R}_1(a,t) = Ur\Psi_F(a)\min(a,t). \tag{72}$$

The second moment equations are $\mathcal{L}_2 = \mathcal{R}_2$ and

$$\mathcal{R}_{2t} + \mathcal{R}_{2a} + \alpha_F \mathcal{R}_2 = 2U\mathcal{R}_1, \qquad \mathcal{S}_{2t} + \mathcal{S}_{2a} + \alpha_S \mathcal{S}_2 = 0, \tag{73}$$

with the $a = 0$ boundary condition that

$$2\mathcal{R}_2(0,t) = \int_0^\infty \alpha_S(a)\mathcal{S}_2(a,t)\,\mathrm{d}a, \qquad \mathcal{S}_2(0,t) = 2\int_0^\infty \alpha_F(a)\mathcal{R}_2(a,t)\,\mathrm{d}a. \tag{74}$$

To obtain the variance in (69) we do not need the complete solution of (73) and (74). Instead, after some judicious integration over $a$, one finds that

$$\frac{\mathrm{d}}{\mathrm{d}t}\langle x^2\rangle = 4U\int_0^\infty \mathcal{R}_1(a,t)\,\mathrm{d}a. \tag{75}$$

Substituting (72) into the result above we obtain

$$\frac{\mathrm{d}}{\mathrm{d}t}\langle x^2\rangle = 4U^2 r\left[\int_0^t a\Psi_F(a)\,\mathrm{d}a + t\int_t^\infty \Psi_F(a)\,\mathrm{d}a\right]. \tag{76}$$

If the right hand side of (76) approaches a constant as $t \to \infty$ then the variance grows diffusively. Otherwise there is anomalous diffusion.

With (76) in hand, one can easily determine if particular models of $\alpha_F$ and $\Psi_F$ lead to anomalous diffusion. For example, with the model in (56), evaluating the integrals in (42) gives a pleasant exact solution

$$\frac{\mathrm{d}}{\mathrm{d}t}\langle x^2\rangle = 4U^2 r\theta_F^2\left[\frac{(1+\tilde{t})^{2-\nu_F}}{(2-\nu_F)(\nu_F-1)} + \frac{1}{(\nu_F-1)(\nu_F-2)}\right], \tag{77}$$

where $\tilde{t} \equiv t/\theta$.

The asymptotic behaviour at large time depends crucially on $\nu_F$. If $\nu_F > 2$ then there is normal diffusion:

$$\frac{\mathrm{d}}{\mathrm{d}t}\langle x^2\rangle \approx \frac{4U^2 r\theta_F^2}{(\nu_F-1)(\nu_F-2)} + O(t^{2-\nu_F})\,. \tag{78}$$

If $1 < \nu_F < 2$, there is superdiffusion

$$\frac{\mathrm{d}}{\mathrm{d}t}\langle x^2\rangle \approx \frac{4U^2 r\theta_F^2 \tilde{t}^{2-\nu_F}}{(2-\nu_F)(\nu_F-1)} + O(1)\,. \tag{79}$$

(At $\nu_F = 2$ there is a logarithmic term.)

Notice the minor role of $\alpha_S(a)$ in the solution above: if $\nu_S > 1$, so that the mean sticking time is finite, then the parameters $\nu_S$ and $\theta_S$ occur only in $r$.

## 4.5 An exercise for the diligent student

Consider an asymmetric two-state model

$$\mathcal{L}_t + \mathcal{L}_a + U_L\mathcal{L}_x + \alpha_L(a)\mathcal{L} = 0, \qquad \mathcal{R}_t + \mathcal{R}_x + U_R\mathcal{R}_x + \alpha_R(a)\mathcal{R} = 0, \tag{80}$$

with the boundary conditions

$$\mathcal{L}(0,t,x) = \int_0^\infty \alpha_R(a)\mathcal{R}(a,t,x)\,\mathrm{d}a, \qquad \mathcal{R}(0,t,x) = \int_0^\infty \alpha_L(a)\mathcal{L}(a,t,x)\,\mathrm{d}a. \tag{81}$$

Show that the average velocity is

$$\bar{U} = \frac{\tau_L U_L + \tau_R U_R}{\tau_L + \tau_R}, \qquad \tau_{L,R} \equiv \int_0^\infty \Psi_{L,R}(a)\,\mathrm{d}a, \tag{82}$$

where $\Psi_L$ and $\Psi_R$ are defined by analogy with (41). Show that the Laplace transform of the velocity autocorrelation function is given by

$$\hat{\mathrm{corr}}(s) = U_{RMS}^2\left[\frac{1}{s} - \frac{\tau_L+\tau_R}{\tau_L\tau_R}\frac{(1-\hat{\psi}_L)(1-\hat{\psi}_R)}{s^2(1-\hat{\psi}_L\hat{\psi}_R)}\right], \tag{83}$$

where

$$U_{RMS}^2 \equiv \frac{\tau_L + \tau_R}{\sqrt{\tau_L \tau_R}} U_R U_L. \tag{84}$$

(If you use the moment method, you will need Laplace transforms to solve the integral equation which arises at $n = 1$.) Using the model

$$\alpha_{R,L}(a) = \frac{\nu_{R,L}}{\theta_{R,L} + a}, \tag{85}$$

perform an asymptotic analysis of (83) to identify the anomalous diffusion exponents which occur if either or both of $\nu_L$ and $\nu_R$ are less than 2.

# 5 Solution of an initial value problem

In this appendix we discuss the issue raised at the end of section 3.1 and analyze a problem in which the death rate of old items is so small that the average lifetime $\tau$ is infinite. For example, this is the case $\nu < 1$ in (42). Specifically, consider the initial value problem posed by (37) with the initial and boundary conditions

$$f(a, 0) = N\delta(a)\,, \qquad f(0, t) = r(t)\,. \tag{86}$$

In (86) the replacement rate $r(t)$ is determined by requiring that

$$N = \int_0^\infty f(a, t)\,\mathrm{d}a\,. \tag{87}$$

The solution of (37) and (86) is

$$f = N\Psi(t)\delta(a - t) + \Psi(a)r(t - a). \tag{88}$$

The first term on the right hand side of the equation above is the cohort of initial items aging and dying. The second term is influx of new items. Imposing (87) on (88), we obtain an integral equation for $r$:

$$N = N\Psi(t) + \int_0^t \Psi(a)r(t - a)\,\mathrm{d}a. \tag{89}$$

The integral relation above is known as the *renewal equation*

Because of the convolution in (89), the Laplace transform

$$[\hat{\Psi}(s), \hat{r}(s)] \equiv \int_0^\infty e^{-sa}[\Psi(a), r(a)]\,\mathrm{d}a\,, \tag{90}$$

is gratifying. In this way we find from (89) that

$$\hat{r} = N\frac{1 - s\hat{\Psi}}{s\hat{\Psi}}. \tag{91}$$

The large-time behaviour of $r(t)$ can be obtained from (91) using standard asymptotic methods.

If $\alpha(a) \propto 1/a$ as $a \to \infty$, then the rightmost singularity of $\hat{\Psi}(s)$in the complex $s$-plane is the branch-point at $s = 0$. We show below in (94) through (97) that the structure of $\hat{\Psi}$ at this branch-point is

$$\Psi(s) = \varpi s^{\nu-1} + \tau + \cdots \tag{92}$$

If $\nu < 1$ then the singular term involving $s^{\nu-1}$ dominates the constant $\tau$ as $s \to 0$. In this case, from(91),

$$\hat{r}(s) \sim \frac{N}{\varpi s^\nu}, \qquad \Rightarrow \qquad r(t) \sim \frac{Nt^{\nu-1}}{\varpi\Gamma(\nu)}, \qquad \text{as} \qquad t \to \infty \tag{93}$$

Because $\nu < 1$ the replacement rate vanishes as $t \to \infty$.

To explain the small-$s$ expansion in (92), we use the model death-rate in (42), which produces the survival function

$$\Psi(a) = \left(\frac{\theta}{\theta + a}\right)^\nu. \tag{94}$$

The Laplace transform in (90) is then

$$\hat{\Psi}(s) = \theta^\nu s^{\nu-1} e^{\theta s}\Gamma(1 - \nu, \theta s), \tag{95}$$

where $\Gamma(a, x)$ is the incomplete $\Gamma$-function defined by Abramowitz & Stegun in their article **6.5.3**. This Laplace transform can be rewritten as

$$\hat{\Psi}(s) = \theta^\nu s^{\nu-1} e^{\theta s}\Gamma(1 - \nu) - \theta\Gamma(1 - \nu)\sum_{n=0}^{\infty}\frac{(\theta s)^n}{\Gamma(2 - \nu + n)}. \tag{96}$$

The form above is convenient because the singular terms containing $s^{\nu-1}$ are localized in the first function on the right hand side. When $s \ll 1$ the expansion of (96) is

$$\hat{\Psi}(s) = \theta^{\nu}\Gamma(1-\nu)s^{\nu-1} + \frac{\theta}{\nu-1} + O(s, s^{\nu}), \tag{97}$$

which is the form assumed in (92).

# References


[1] D.D. Joseph and L. Preziosi. Heat waves. *Rev. Mod. Phys.*, 61:41–73, 1989.

[2] M. Schlesinger, G.M. Zaslavsky, and U. Frisch. *Lévy Flights and Related Topics in Physics*. Springer, Berlin, 1994.

[3] T.H. Solomon, E. Weeks, and H.L. Swinney. Chaotic advection in a two-dimensional flow: Lévy flights and anomlaous diffusion. *Physica D*, 76:70–84, 1994.

[4] G.I. Taylor. Diffusion by continuous movements. *Proc. London Math. Soc.*, 20:196–212, 1921.

[5] E.R. Weeks, J.S. Urbach, and H.L. Swinney. Anomalous diffusion in asymmetric random walks with a quasi-geostrophic example. *Physica D*, 97:291–310, 1996.